Theory of the Collapsing Axisymmetric Cavity

J. Eggers,[1] M. A. Fontelos,[2] D. Leppinen,[3] and J. H. Snoeijer[1]

[1]School of Mathematics, University of Bristol, University Walk, Bristol BS8 1TW, United Kingdom
[2]Departamento de Matemáticas, Consejo Superior de Investigaciones Científicas, C/Serrano 123, 28006 Madrid, Spain
[3]School of Mathematics, University of Birmingham, Edgbaston Birmingham B15 2TT, United Kingdom

(Received 18 October 2006; published 1 March 2007)

We investigate the collapse of an axisymmetric cavity or bubble inside a fluid of small viscosity, like water. Any effects of the gas inside the cavity as well as of the fluid viscosity are neglected. Using a slender-body description, we compute the local scaling exponent $\alpha = d\ln h_0/d\ln t'$ of the minimum radius h_0 of the cavity, where t' is the time from collapse. The exponent α very slowly approaches a universal value according to $\alpha = 1/2 + 1/[4\sqrt{-\ln(t')}]$. Thus, as observed in a number of recent experiments, the scaling can easily be interpreted as evidence of a single nontrivial scaling exponent. Our predictions are confirmed by numerical simulations.

DOI: 10.1103/PhysRevLett.98.094502 PACS numbers: 47.55.df, 02.40.Xx, 47.15.K−

Over the last decade, there has been considerable progress in understanding the pinchoff of fluid drops, described by a set of universal scaling exponents, independent of the initial conditions [1,2]. The driving is provided for by surface tension; the value of the exponents depends on the forces opposing it: inertia, viscosity, or combinations thereof. Bubble collapse appears to be a special case of an inviscid fluid drop breaking up inside another inviscid fluid, which is a well studied problem [3–5]: the minimum drop radius scales like $h_0 \propto t'^{2/3}$, where $t' = t_0 - t$ and t_0 is the pinch-off time. Thus, huge excitement was caused by the results of recent experiments on the pinchoff of an air bubble [6–10], or the collapse of a cavity [11] in water, which resulted in a radically different picture, in agreement with two earlier studies [12,13]. As demonstrated in detail in [10], the air-water system corresponds to an inner "fluid" of vanishing inertia, surrounded by an ideal fluid.

Firstly, the scaling exponent α, obtained from the slope of a log-log plot over a range of up to 3 decades, was found to be close to $1/2$, (typical values reported in the literature are 0.56 [9] and 0.57 [10]). This means that breakup is much faster than in the fluid-fluid case, and surface tension must become irrelevant as a driving force. Secondly, the value of α appeared to depend subtly on the initial condition [11], and was typically found to be larger than $1/2$. This raised the possibility of an "anomalous" exponent, selected by a mechanism as yet unknown. To illustrate the qualitative appearance of the pinchoff of a bubble, in Fig. 1 we show a temporal sequence of profiles, using a full numerical simulation of the inviscid flow equations [5]. We confine ourselves to axisymmetric flow, which experimentally is found to be preserved down to a scale of a micron [10], provided the experiment is aligned carefully [9].

The only existing theoretical prediction [7,11,14] is based on treating the bubble as a (slightly perturbed) cylinder [12,13], which leads to the exponent being $1/2$ with logarithmic corrections. Very similar analyses have been performed since the 1940's [15,16] for the shape of a cavity behind a moving body. Owing to the constant speed of convection, the cavity shape swept out by the body directly corresponds to time dependence of the cylinder, giving the same answer if the distance from the body is interpreted as the time distance from the singularity. Our numerics, to be reported below, are however inconsistent with [7,11,14]. Moreover, a cylinder is not a particularly good description of the actual profiles (cf. Figure 1), as has been remarked before [9]. In this Letter, we present a systematic expansion in the slenderness of the cavity, which is found to lead to a self-consistent description of pinchoff. Our results are in excellent agreement with numerical simulations, and consistent with the experimentally observed exponents.

Our approach is based on the slenderness of the cavity [16,17], an assumption we confirm later. The inviscid, irrotational, incompressible flow $\mathbf{u} = \nabla\phi$ outside the cavity of length $2L$ is written as

$$\phi = \int_{-L}^{L} \frac{C(\xi, t)d\xi}{\sqrt{(z-\xi)^2 + r^2}}, \tag{1}$$

where $C(\xi, t)$ is a line distribution of sources to be deter-

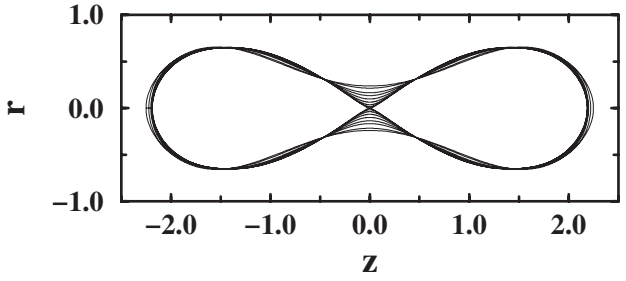

FIG. 1. Numerical simulation of the time evolution of bubble pinchoff from initial conditions given by the shape with the largest waist. Pinchoff is initiated by surface tension, but the late stages are dominated by inertia, as observed experimentally [10].

mined. The length L will later drop out of the description of the pinch region, where (1) is good. For a slender geometry, $\partial_z\phi \ll \partial_r\phi$, so the radial velocity u_r dominates. The latter, evaluated at the cavity wall, is found from taking the derivative of (1) with respect to r and setting $r = h(z, t)$. The leading contribution to the resulting integral [17] is local: $|\xi - z| \lesssim h$, thus in a slender description $C(\xi, t) \approx C(z, t)$ and $L \to \infty$. With these approximations, the ξ-integration can be performed exactly, giving $u_r \approx -2C(z, t)/h(z, t)$.

From the kinematic condition, the cavity radius $h(z, t)$ is related to u_r by $\partial_t h \approx u_r$, and thus $\dot{a}(z, t) \approx -4C(z, t)$, where $a = h^2$ and the dot denote the time derivative. Finally, an equation of motion for C comes from the Bernoulli equation [18], with the pressure p set to zero at infinity. Since the pressure difference $p_0 - p$ across the interface is the Laplace pressure $\gamma\kappa$, we arrive at

$$\int_{-L}^{L} \frac{\ddot{a}(\xi, t)d\xi}{\sqrt{(z - \xi)^2 + a(z, t)}} = \frac{\dot{a}^2}{2a} - \frac{4\gamma}{\rho}\kappa + \frac{4p_0}{\rho}, \quad (2)$$

where p_0 is the cavity pressure [19]. In the two-fluid problem, the surface tension γ, multiplied by the mean curvature $\kappa \approx 1/h$, drives the problem. However, in our problem, breakup is much faster, so the last two terms in (2) can be neglected asymptotically. The resulting equation is invariant under a rescaling of both space and time, as both remaining terms are inertial (describing acceleration and convection of a fluid element); thus, scaling exponents are not fixed by dimensional analysis. Note that (2) does not conserve the volume of the cavity, whereas Fig. 1 assumes an incompressible gas inside the bubble. This however only affects the rounded ends of the bubble.

Our aim is to explain the observed scaling behavior of the minimum cross section $a_0 = a(0, t)$, as well as of the axial length scale Δ of the profile, which can be characterized by the inverse curvature $\Delta \equiv (2a_0/a_0'')^{1/2}$, where $a_0'' = a''(0, t)$ and the prime denotes a derivative with respect to z. Experiments [11] as well as our own simulations show that the aspect ratio a_0/Δ^2 becomes small for $t' \to 0$. This means that $a(0, t)$ can be neglected relative to $\xi^2 \approx \Delta^2$ in the denominator of the integral in (2), except near the position $\xi = 0$ of the minimum. Thus since the integral is dominated by *local* contributions near the minimum, we can find equations of motion for the minimum in terms of local quantities alone.

As shown later, $\ddot{a}(\xi, t)$ goes to zero over the axial scale Δ; hence, $\ddot{a}(\xi, t) \approx \ddot{a}_0$ up to terms of order Δ^2. Thus the integral in (2), evaluated at $z = 0$, can be approximated as

$$\ddot{a}_0 \int_{-\Delta}^{\Delta} [\xi^2 + a_0]^{-1/2} d\xi = \ddot{a}_0 \ln(4\Delta^2/a_0) + O\left(\frac{a_0}{\Delta^2}\right).$$

An arbitrary factor inside the logarithm depends on the exact shape of $\ddot{a}(\xi, t)$, but is irrelevant for the asymptotic limit. We now need another equation for the (time-dependent) width Δ to close the description. To that end, we evaluate the second derivative of (2) at $z = 0$.

The contribution of the left hand side of (2) is

$$\int_{-\Delta}^{\Delta} \ddot{a}(\xi, t)\left[\frac{2\xi^2 - a_0}{\sqrt{\xi^2 + a_0}5} - \frac{a_0''}{2\sqrt{\xi^2 + a_0}3}\right]d\xi.$$

For a slender profile, a_0'' is subdominant, but the integral over the first term in angular brackets conspires to give zero in the limit $a_0 \to 0$, so the second term has to be considered as well, and $\ddot{a}(\xi, t)$ has to be expanded beyond the constant term: $\ddot{a}(\xi, t) = \ddot{a}_0 + \ddot{a}_0''\xi^2/2$. Thus, using the same reasoning as before, and keeping in mind that $a_0' = 0$, we find for the second derivative of the integral

$$\int_{-\Delta}^{\Delta} \left[\frac{(\ddot{a}_0 + \ddot{a}_0''\xi^2/2)(2\xi^2 - a_0)}{\sqrt{\xi^2 + a_0}^5} - \frac{\ddot{a}_0 a_0''}{2\sqrt{\xi^2 + a_0}^3}\right]d\xi \approx \left[\ddot{a}_0'' \ln\left(\frac{4\Delta^2}{e^3 a_0}\right) - 2\frac{\ddot{a}_0 a_0''}{a_0}\right].$$

Equating this with the second derivative of the right hand side of (2), $[\dot{a}^2/(2a)]''$, which is readily computed in terms of a_0 and Δ, yields the desired second equation. It is slightly more convenient to rewrite the results as equations for the local (time-dependent) exponents

$$2\alpha \equiv -\partial_\tau a_0/a_0, \qquad 2\delta \equiv -\partial_\tau a_0''/a_0'', \quad (3)$$

where $\tau \equiv -\ln t'$ and $\beta = \alpha - \delta$. Note that (3) is equivalent to taking the slope of a log-log plot, but differs from $h_0 \propto t'^{\alpha}$ if α is time-dependent. The result is

$$(\alpha_\tau + \alpha - 2\alpha^2)\ln(\Gamma_1/a_0'') = -\alpha^2, \quad (4)$$

$$(\delta_\tau + \delta - 2\delta^2)\ln(\Gamma_2/a_0'') = 2\alpha - 3\alpha^2 - 2\alpha\delta + 2\alpha_\tau, \quad (5)$$

where the subscript denotes the τ-derivative.

The scaling factors Γ_1, Γ_2 only make a subdominant contribution as a_0'' goes to zero. The time dependence of a_0'' is found from integrating

$$\ln(a_0'')_\tau = -2\delta. \quad (6)$$

The approach of the exponents toward their fixed point value $(\alpha, \delta) = (1/2, 0)$ is given by an expansion of (4) and (6) in powers of $\tau^{-1/2}$, fractional powers providing the right balance:

$$\alpha = 1/2 + \frac{1}{4\sqrt{\tau}} + \frac{\Gamma}{\tau} + O(\tau^{-3/2}),$$
$$\delta = \frac{1}{4\sqrt{\tau}} + O(\tau^{-3/2}). \quad (7)$$

The constant Γ depends on the values of Γ_1 and Γ_2. The next order changes with the choice of time scale (which is not fixed by (2)), and thus necessarily depends on the initial conditions. Below, we present numerical evidence that Γ_1 and Γ_2 are universal, and we hope to be able to calculate

their values in the future. At that point, it will become expedient to study the system of (4)–(6) in more detail, beyond the expansion (7). As seen from (7), the leading order α and β approach their limiting values of $1/2$ in a *universal* fashion. For the self-consistency of our analysis, we need for the dimensionless parameter a_0'' to go to zero toward pinchoff, as is indeed found from (6), owing to the slowness with which δ converges toward zero.

We now turn to a detailed comparison with full numerical simulations, not relying on any slenderness assumption, by focusing on the late stages of the pinch-off event shown in Fig. 1. To this end, a suitably modified version of the boundary integral code developed to examine inviscid droplet pinchoff [5] was used, as originally reported in [20]. This involved two important modifications: First, the boundary value operator (cf. Equation (11) in [5]) has a zero eigenvalue in the case of the absence of an inner fluid, corresponding to a change in the bubble volume. This singularity is analytically removed before the boundary integral operator is inverted, fixing the bubble volume. Second, due to the rapidity of bubble pinchoff, the adaptive time stepping used for droplet pinchoff in [5] was replaced by a time-step halving procedure with error estimation.

A comparison of the numerical simulations with (7) is given in Fig. 2. Using Eq. (3), the value of α from the numerical simulations can be calculated as $\alpha = t'\partial_{t'}h_0/h_0$, and the pinch-off time t_0 is estimated directly from the numerical data, without an attempt to improve the agreement with theory. The solid curve in Fig. 2 is the data from the numerical simulation, and the dashed curve is the leading order prediction given by Eq. (7) with $\Gamma = 0$.

Data from the numerical simulations can be divided into three regimes. From approximately $10^{-12} < t' < 10^{-4}$, the bubble is considered to be in the asymptotic regime, and it is seen that there is very good agreement between the numerical data and the asymptotic theory: the leading order theory with $\Gamma = 0$ accurately predicts the extremely slow decrease in the numerically determined value of α.

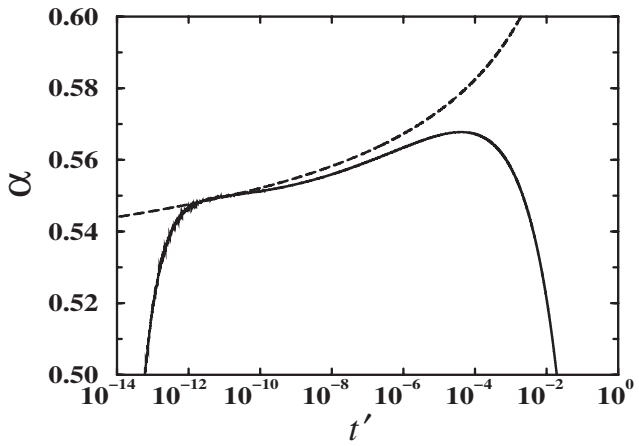

FIG. 2. A comparison of the exponent α between full numerical simulations of bubble pinchoff (solid line) and the leading order asymptotic theory with $\Gamma = 0$ (dashed line).

Equally good agreement was found for numerical runs using other initial conditions. Time $t' > 10^{-4}$ corresponds to a transitional regime where the bubble adjusts from an initial state where surface tension is required to initiate pinchoff, to an asymptotic state where surface tension is irrelevant. Time $t' \sim 10^{-12}$ represents the threshold of the numerical simulations: extremely large interfacial velocities acting over ever-decreasing length scales, ultimately puts a limit on the validity of the numerical simulations.

Gordillo *et al.* [7,14] have previously predicted that the minimum bubble radius h_0 should scale with t' according to $t' \propto h_0^2\sqrt{-\ln h_0^2}$, using a method that in many respects is similar to ours [14]. However, the crucial difference is that they do not treat the axial length scale Δ as a dynamical variable as we do, but effectively identify Δ with some outer length scale. Indeed, if one replaces a_0'' by a_0 in (4), one recovers the scaling result of [14]. The conceptual difference between the two approaches is illustrated further by Fig. 3, which shows the central peak of $\ddot{a}$ from the full numerical simulation. The value of $\ddot{a}$ rapidly drops to zero, effectively providing the cutoff of the integral (2) at an axial length Δ. Computations using different initial conditions, evaluating $\ddot{a}$ at different times, show collapse upon rescaling, indicating self-similar behavior of the entire profile. So far, we have not been able to identify the logarithmic corrections of β in our full numerical simulations, since computing the axial scale is much more demanding than computing h_0.

In Fig. 4, we plotted the numerically computed minimum radius h_0, divided by the universal part of the present theory (full line) and that of [14] (dashed line). If normalized by an appropriate constant, the result should be unity. Namely, (7) with $\Gamma = 0$ is equivalent to $h_{0,\mathrm{pred}} \propto t'^{1/2}\sqrt{e^{-\sqrt{-\ln t'}}}$ (as calculated from (3)), while the theory

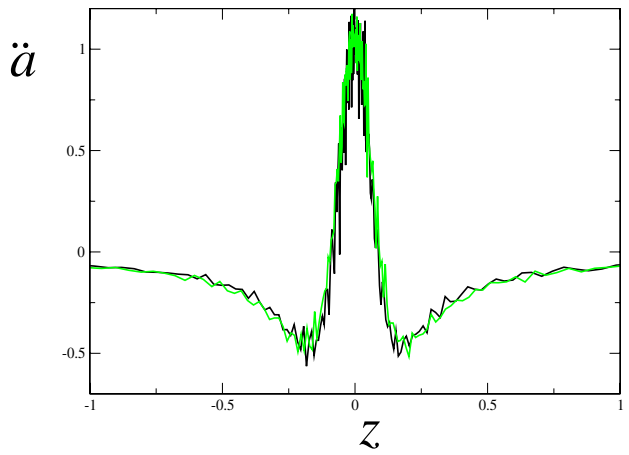

FIG. 3 (color online). A normalized graph of $\ddot{a} = \partial^2 h^2(z,t)/\partial t^2$ as given by the full numerical simulations, for two different initial conditions, and at $t' = 3.8 \times 10^{-10}$ (black line) and $t' = 2.1 \times 10^{-10}$ (grey line, green online). Similar collapse is found if profiles are evaluated at different times for the same initial conditions.

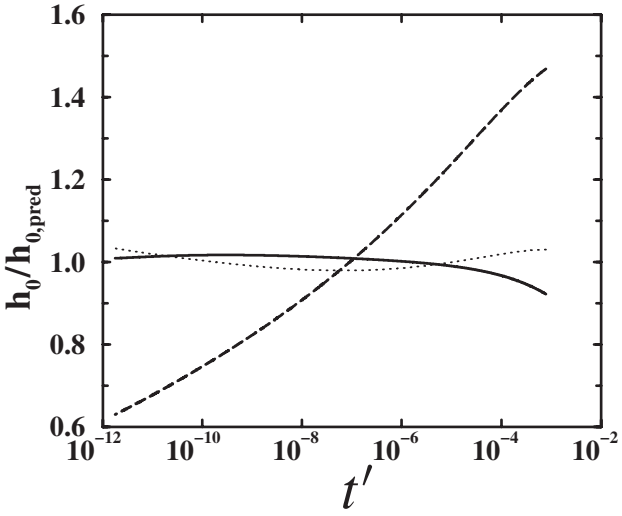

FIG. 4. A normalized graph of $h_0/h_{0,\mathrm{pred}}$, where (i) $h_{0,\mathrm{pred}} \propto t'^{1/2}/(-\ln h_0^2)^{1/4}$ (dashed line), (ii) $h_{0,\mathrm{pred}} \propto t'^{\bar{\alpha}}$ (dotted line), and (iii) $h_{0,\mathrm{pred}} \propto t'^{1/2}\sqrt{e^{-\sqrt{-\ln t'}}}$ (solid line).

of [7,14] (equation (2.30) in [14]) corresponds to $h_{0,\mathrm{pred}} \propto t'^{1/2}/(-\ln h_0^2)^{1/4}$. While the present theory agrees extremely well with numerics without the use of any adjustable constant, the theory in [14] varies by approximately $\pm 50\%$ over the range of t' plotted.

In our earlier numerical simulations [20], as well as in most experimental papers [6,9,10], the data for the minimum radius was represented by adjusting a single exponent $\bar{\alpha}$. Although Fig. 2 clearly shows that the exponent is slowly varying, this subtle feature is difficult to detect in a more conventional plot like Fig. 4. To demonstrate this point, we have determined an effective exponent $\bar{\alpha} = 0.559$ from a least-square fit to the numerical data, a value which is close to those observed experimentally [9,10]. In essence, $\bar{\alpha}$ can be viewed as the average over α values shown in Fig. 2. The resulting fit (dotted line) gives a surprisingly good description of the data, as a result of the extremely slow variation of α. It also highlights the need for more sophisticated plots like Fig. 2 in the interpretation of future (experimental) data.

To summarize, we have developed an asymptotic theory for the collapse of an axisymmetric cavity. A novel feature of this theory is a slow variation of the scaling exponents, whose leading order contributions are universal. The slowness of the approach explains the experimental observation of apparently new scaling exponents, whose value may depend weakly on initial conditions. It remains to calculate the entire form of the central peak of $\ddot{a}$, which according to Fig. 3 is universal. This will determine the values of the constants Γ_1 and Γ_2. Other challenges are the inclusion of nonaxisymmetry [9] and viscosity [10] into the theoretical description.

We thank J. Lister for his continued support, valuable insight, and very detailed comments on the manuscript, as well as J. M. Gordillo for discussions. S. Thoroddsen made his experiments available to us prior to publication, for which we are grateful. J. H. S. acknowledges financial support from a Marie Curie European Grant FP6 (No. MEIF-CT2006-025104).

[1] J. Eggers, Rev. Mod. Phys. **69**, 865 (1997).
[2] J. Eggers, Z. Angew. Math. Mech. **85**, 400 (2005).
[3] Y. J. Chen and P. H. Steen, J. Fluid Mech. **341**, 245 (1997).
[4] R. F. Day, E. J. Hinch, and J. R. Lister, Phys. Rev. Lett. **80**, 704 (1998).
[5] D. Leppinen and J. R. Lister, Phys. Fluids **15**, 568 (2003).
[6] J. C. Burton, R. Waldrep, and P. Taborek, Phys. Rev. Lett. **94**, 184502 (2005).
[7] J. M. Gordillo *et al.*, Phys. Rev. Lett. **95**, 194501 (2005).
[8] S. T. Thoroddsen, T. G. Etoh, and K. Takehara, Bull. Am. Phys. Soc. **50**, BD.00002 (2005).
[9] N. C. Keim *et al.*, Phys. Rev. Lett. **97**, 144503 (2006).
[10] S. T. Thoroddsen, T. G. Etoh, and K. Takehara, Phys. Fluids (to be published).
[11] R. Bergmann *et al.*, Phys. Rev. Lett. **96**, 154505 (2006).
[12] M. S. Longuet-Higgins, B. R. Kerman, and K. Lunde, J. Fluid Mech. **230**, 365 (1991).
[13] H. N. Oguz and A. Prosperetti, J. Fluid Mech. **257**, 111 (1993).
[14] J. M. Gordillo and M. Pérez-Saborid, J. Fluid Mech. **562**, 303 (2006).
[15] N. Levinson, Ann. Math. **47**, 704 (1946).
[16] V. V. Serebryakov, Dokl. Akad. Nauk Ukr. SSR, Ser. A. **12**, 1119 (1973).
[17] E. J. Hinch, *Perturbation Methods* (Cambridge University Press, Cambridge, 1991).
[18] L. D. Landau and E. M. Lifshitz, *Fluid Mechanics* (Pergamon, Oxford, 1984).
[19] Equation (2), as it stands, is however ill-posed. Namely, if $a(z, t)$ in the denominator of the integral operator is assumed constant, the operator can be inverted by Fourier transform. One finds that the high-wave number modes of $\ddot{a}$ grow like $\exp(k\sqrt{a})$, so the evolution (2) will soon be polluted by short-wavelength noise. However, this problem can be dealt with completely by adding a small "damping" term $\epsilon\ddot{a}''a$ to the right hand side. Choosing $\epsilon = 10^{-3}$, we find that the evolution is completely stable, yet the damping term and its derivatives is always uniformly smaller than the other terms by more than 4 orders of magnitude.
[20] D. Leppinen, J. R. Lister, and J. Eggers, Bull. Am. Phys. Soc. **50**, BD.00006 (2005).